CHINESE OPTICS LETTERS

Vol. 20, No. 7 | July 2022

High repetition rate actively mode-locked Er:fiber laser with tunable pulse duration

Gang Yao (姚 港)[1], Zhigang Zhao (赵智刚)[1,2], Zhaojun Liu (刘兆军)[1], Xibao Gao (高悉宝)[1], and Zhenhua Cong (丛振华)[1*]

[1] School of Information Science and Engineering, and Shandong Provincial Key Laboratory of Laser Technology and Application, Shandong University, Qingdao 266237, China

[2] State Key Laboratory of Quantum Optics and Quantum Optics Devices, Shanxi University, Taiyuan 030006, China

*Corresponding author: congzhenhua@sdu.edu.cn

Received January 4, 2022 | Accepted April 22, 2022 | Posted Online May 24, 2022

An actively mode-locked fiber laser with controllable pulse repetition rate and tunable pulse duration is presented, in which an optical delay line (ODL) is used to adjust the cavity length precisely for regulating the repetition rate, and a semiconductor optical amplifier (SOA) is introduced for enabling the pulse duration control. Experimentally, continuous tuning of the repetition rate from 2 GHz to 6 GHz is realized, which is limited by the availability of an even higher repetition rate radio-frequency (RF) source. Specifically, when the repetition rate is fixed at 2.5 GHz, the pulse duration can be tuned from 4 ps to 30 ps, which is, to the best of our knowledge, the widest tuning range of pulse duration ever achieved in a gigahertz (GHz) repetition rate actively mode-locked 1.5 μm fiber laser oscillator.

Keywords: active mode-locking; semiconductor optical amplifier; tunable pulse duration; high repetition rate.
DOI: 10.3788/COL202220.071402

1. Introduction

Ultra-short pulse lasers with high repetition rates are widely used in nonlinear frequency conversion, lidar, optical frequency combs, and material micro-processing[1–4]. Thus far, mode-locking has been well understood and developed as an important method for the generation of ultra-short optical pulses, including passive mode-locking and active mode-locking. Comparatively speaking, passive mode-locking is simpler in structure and can be realized by both real absorbers[5,6] and Kerr-effect-based artificial saturable absorbers[7], with which, however, it is not that easy to generate ultra-high repetition rate ($>$ 1 GHz) pulses because of the requirement of very short cavity length, although it is not impossible. In contrast, active mode-locking is more straight-forward for high repetition rate generation, which usually works at the harmonic mode-locking state and is based on the employment of electro-optical modulators or acoustic-optical modulators. In addition, the pulse repetition rate can be tunable and controlled by the adopted radio-frequency (RF) sources.

However, tuning of the pulse duration is not easy in approximately gigahertz (GHz) actively mode-locked fiber lasers. In active mode-locked lasers, there are usually three ways to tune the pulse width, one of which is detuning the repetition rate of the laser from the repetition rate of the RF source. For example, Qin *et al.* reported linear pulse width tuning from 310 ps to 1 ns in the case of the fundamental frequency (14.6 MHz) by precisely adjusting the degree of detuning[8], in which, however, the pulse repetition rate also changes with the detuning frequency. The second way is to adjust the pulse width of the RF signal. Chen *et al.* reported changing of pulse width from 33 ps to 910 ps at the fundamental frequency of 13.12 MHz[9], which, however, has higher requirements for the modulation signal source and does not work well when the harmonic order increases. A tuning range of just a few picoseconds could be realized when the repetition rate was at 6.2 GHz. Except for that, the third method is the introduction of other devices into the cavity for pulse width tuning, such as the semiconductor optical amplifier (SOA), which is a commonly used device in actively mode-locked lasers. It can be directly used as an electro-optical modulator or as an opto-optical modulator in optical injection actively mode-locked lasers[10–16]. The nonlinear effects in SOA, such as nonlinear polarization rotation (NPR) and cross gain modulation (XGM), enable itself to be used not only for passively mode-locked lasers[17], but also to improve the pulse quality in actively mode-locked lasers[18–22]. There are two options for using SOA to tune the pulse duration. One is to use XGM in SOA to build an optical injection mode-locked laser, and the other one is to directly insert the SOA into the laser cavity. In the optical injection SOA fiber laser, the pulse width can be adjusted by changing the waveform of the injected light, and the pulse width adjustment of 12–15 ps has been realized[14]. SOA can be used to

realize pulse width tuning in electro-optic modulated actively mode-locked lasers. For example, by varying the driving current of SOA in an erbium-doped fiber (EDF) ring laser, the pulse width changing from 12 ps to 16 ps was achieved[19]. There are also reports on theoretical research on the influence of SOA on pulse width[23–25]. However, these pulse width tunings using SOA have a small range of only a few picoseconds, which is quite limited. To the best of our knowledge, there is no report on pulse duration tunable ~GHz actively mode-locked fiber lasers.

In this Letter, an actively mode-locked laser with tunable pulse repetition rate and pulse width is demonstrated. The repetition rate of the fiber laser is able to tune from 2 GHz to 6 GHz by adjusting the optical delay line (ODL) and RF signal generator. Besides, the pulse width can be continuously tuned within the range from 4 ps to 30 ps at the repetition rate of 2.5 GHz by using the NPR in the SOA and the polarization sensitivity of the lithium niobate ($LiNbO_3$) intensity modulator. The output power is increased from 7 mW to 24 mW due to the change in the SOA input current.

2. Experiment Setup

The schematic diagram of the experimental setup of the high repetition rate pulse width tunable actively mode-locked fiber laser is illustrated in Fig. 1. A wavelength-stabilized 976 nm single-mode fiber coupled laser diode was used as pump source, and the gain medium was a piece of 50-cm-long EDF (Liekki, Er-110). A polarization-independent isolator was used to ensure the unidirectional laser operation. A $LiNbO_3$ Mach–Zehnder intensity modulator (MZIM) was driven by a signal generator with adjustable RF ranging from 0 GHz to 6 GHz (SRS SG386). A polarization controller (PC) was inserted before the MZIM to control the polarization state of the laser light entering the modulator. An SOA (Thorlabs, SOA1117S) was utilized to control the pulse width. The cavity length can be regulated by an ODL with a maximum delay time of 500 ps. A 1545 nm bandpass filter with a 3 dB bandwidth of 1.4 nm was used to select the target wavelength. Finally, the pulse was coupled out by a 3 dB coupler.

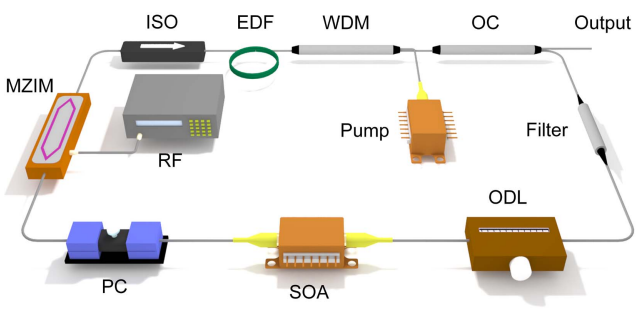

Fig. 1. Schematic diagram of the experimental setup of the actively mode-locked fiber laser. MZIM, Mach–Zehnder intensity modulator; RF, radio-frequency signal generator; ISO, isolator; EDF, erbium-doped fiber; WDM, wavelength division multiplexer; OC, optical coupler; ODL, optical delay line; SOA, semiconductor optical amplifier; PC, polarization controller.

3. Result and Discussion

ODL plays a key role in repetition rate management by adjusting the cavity length, which can be changed from about 16.5 m to 16.65 m, corresponding to fundamental repetition rates of 12.42 MHz and 12.54 MHz, respectively. Experimentally, it is necessary to adjust both modulation frequency and cavity length of the cavity to enable the continuous tuning of the pulse repetition rate, by which the output repetition rate equals an integer multiple of the fundamental repetition rate. Meanwhile, ODL can also improve the short-term stability of the actively mode-locked laser system by precisely matching the cavity length to the modulation frequency. Figure 2 shows the phase noise at the repetition frequency of 2.5 GHz. It can be seen from the figure that after ODL precisely controls the cavity length the phase noise is −60.84 dBc/Hz at the offset frequency of 10 Hz, and the phase noise is −113.87 dBc/Hz at the offset frequency of 1 MHz. After calculation, the jitter is 0.373 ps. Figures 3(a1)–3(f1) show the mode-locked pulse trains at the repetition rates of 1 GHz, 2.5 GHz, and 6 GHz, respectively, which were detected and recorded by a high-speed photodetector (New Focus, 1554-B, 12 GHz) and an oscilloscope (Keysight, DS090804A, 8 GHz). To achieve ultra-high repetition rates, the actively mode-locked laser operated at the harmonic mode-locking state. The corresponding harmonic orders of the pulse trains in Fig. 3 are 80th, 200th, and 480th, respectively.

In fact, SOA is multi-functional in this experiment. Firstly, SOA is responsible for the pulse width tuning. Secondly, due to gain saturation of SOA, the main mode consumes most of the carriers, which reduces the gain of the side mode, thus reducing super-mode noise[19,26]. Also, part of the gain in the cavity is provided by the SOA. During the pulse width tuning process, the ODL is changed to keep the laser in a stable mode-locked state, and, then, the input current of the SOA is adjusted to 500 mA. The minimum pulse width can be obtained by rotating the PC carefully. Afterwards, the pulse width was controllable by changing the input current of the SOA. As shown in Figs. 3(a2)–3(f2), autocorrelation curves are measured by autocorrelators

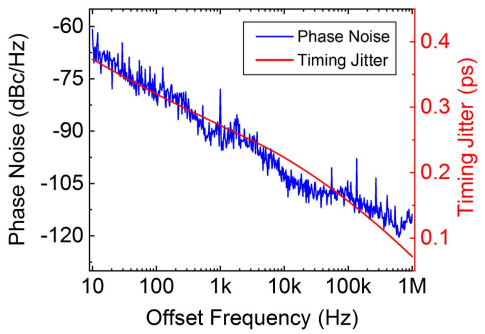

Fig. 2. Phase noise when the repetition rate is 2.5 GHz and the pulse width is 4 ps.

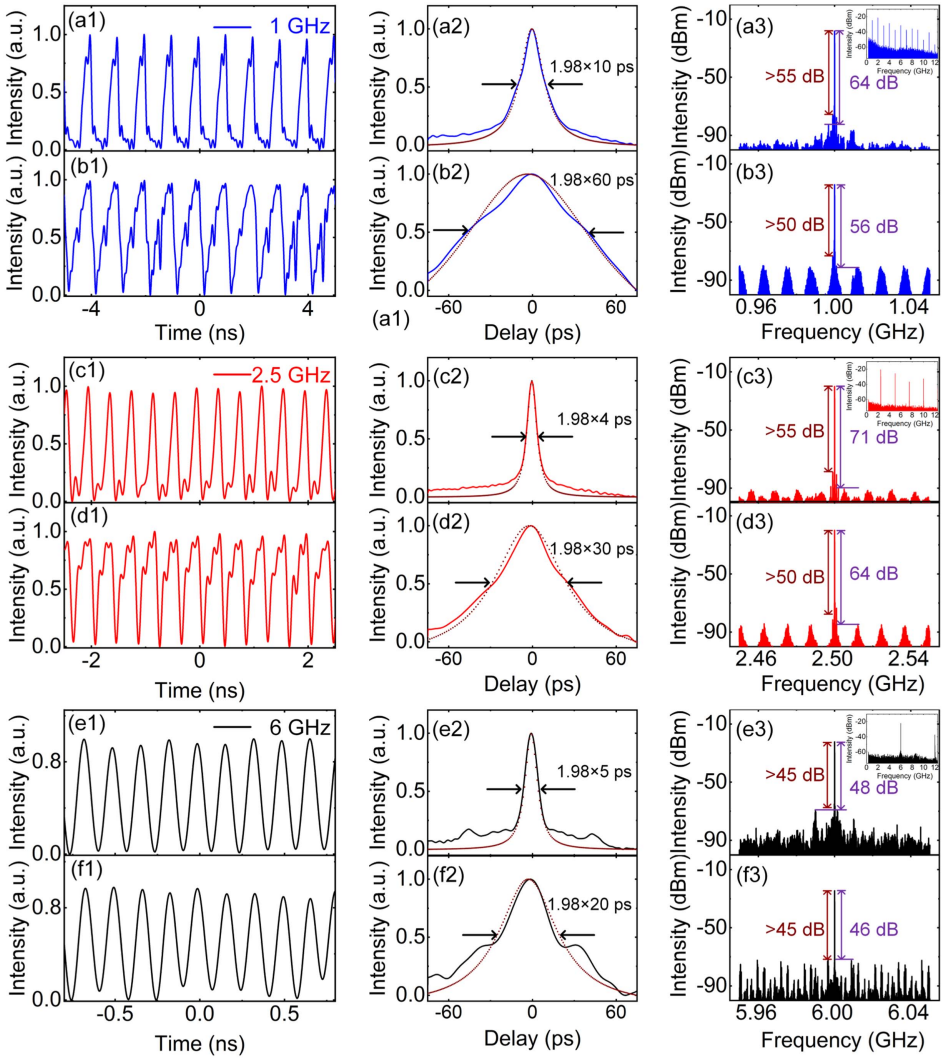

Fig. 3. Output pulse trains of the laser with repetition rate and SOA current of (a1) 1 GHz, 500 mA, (b1) 1 GHz, 174 mA, (c1) 2.5 GHz, 500 mA, (d1) 2.5 GHz, 174 mA, (e1) 6 GHz, 500 mA, (f1) 6 GHz, 260 mA, (a2)–(f2) the corresponding pulse width fitting curve, and (a3)–(f3) the corresponding RF spectra.

(APE-Pulsecheck) under different SOA currents and different repetition rates. At the 1 GHz repetition rate, the pulse width increases from 10 ps to 60 ps as the SOA current decreases from 500 mA to 174 mA. Similarly, the pulse width is increased from 4 ps to 30 ps at the 2.5 GHz repetition rate with a 326 mA reduction in SOA current. Limited by the gain in the cavity, Figs. 3(f1)–3(f3) show parameters measured at 260 mA, which is the minimum SOA current that can generate pulses at 6 GHz. The pulse width at this current is 20 ps. The higher threshold current is also the reason why the pulse width tuning range is only 15 ps at the 6 GHz repetition rate. Figure 4 shows the autocorrelation curve of pulse width of different SOA currents at 2.5 GHz repetition rate under the same PC condition, which also proves that the pulse width varies continuously with SOA current.

Figure 3 also shows the waveform and RF spectrum of different SOA currents at different repetition rates. By comparing Figs. 3(a1) and 3(b1), it can be seen that the pulse waveform expands significantly with the increase of pulse width, which can also be seen in Figs. 3(c1) and 3(d1). It should be noted that the 6 GHz waveforms shown in Figs. 3(e1) and 3(f1) are not real waveforms because the bandwidth of the oscilloscope is 8 GHz. Figures 3(a3)–3(f3) show the RF spectra corresponding to each repetition rate and pulse width. As shown in these figures, the pulse signal-to-noise ratio (SNR) is higher than 45 dB. In addition, due to the noise reduction capabilities of the SOA, the SNR is relatively small at low SOA currents, as is the side mode rejection ratio (SMR). When the repetition rate is 1 GHz, the SMR increases from 56 dB to 64 dB with the increase of SOA current. Similarly, the SMR also increases by 7 dB and 2 dB at the repetition rates of 2.5 GHz and 6 GHz, which also verifies that SOA shows different levels of super-mode noise suppression capabilities under different currents[17,27].

As the pulse width varies, the spectrum also changes. Figure 5 shows the relationship between the spectra and the SOA currents under the same PC condition at a repetition rate of

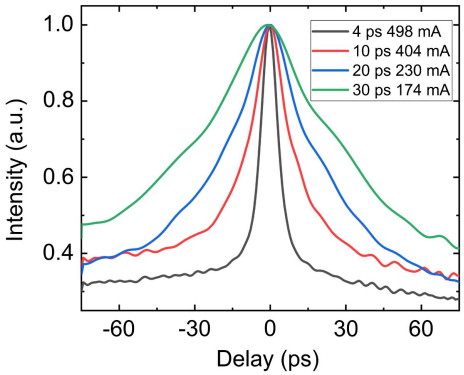

Fig. 4. Autocorrelation curves of different SOA currents at the repetition rate of 2.5 GHz.

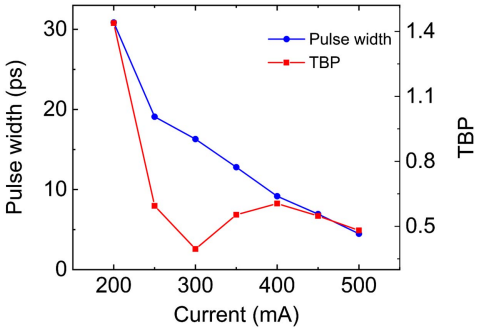

Fig. 6. Pulse width and TBP at different SOA currents.

2.5 GHz. The spectrum is characterized by an optical spectrum analyzer (Yokogawa Q6370D). When the current of the SOA is 500 mA, the 3 dB spectral width is the widest, which is 0.85 nm. When the current decreased, the laser changed from dual-wavelength mode-locking to single-wavelength mode-locking, as shown by the green line in Fig. 5, and the spectral bandwidth was also reduced, which may be due to the enhancement of mode competition. SOA is an inhomogeneous broadening medium that can inhibit super-model competition. But, SOA does not provide sufficient gain to suppress super-model noise at low current. When the spectral bandwidth was reduced to 0.19 nm at 300 mA current, it started to increase again and finally became 0.37 nm at the current of 200 mA. During this process, a slight red shift of the center wavelength also occurred, for which the refractive index changes in the SOA should be responsible[23,25,28].

The variations in pulse width and bandwidth also bring changes to the time bandwidth product (TBP). Figure 6 shows the pulse width and TBP for different input SOA currents at the 2.5 GHz repetition rate. When the current is higher than 250 mA, the change trend of pulse width is approximately linear, and the variation of TBP is small. However, at the current of 200 mA, the pulse width is widened rapidly, and the spectral bandwidth is stretched as well, resulting in the rapid increase of TBP to 1.44, which indicates the existence of a large number of chirps at 200 mA. In fact, in the process of pulse width tuning,

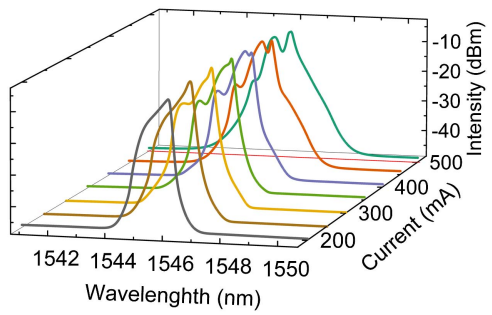

Fig. 5. Spectra of the laser at different SOA currents at the repetition rate of 2.5 GHz.

the TBP of pulse is greater than the Lorentz fitting pulse transformation limit of 0.142, which indicates that the output pulses exhibit different chirp at different SOA input currents. This phenomenon is caused by the dynamic chirp of SOA[29]. The chirp of SOA is usually negative and can be used to compensate intracavity positive chirp[30,31]. When the current is less than 250 mA, the SOA cannot work properly. The effect on the pulse is to produce a lot of chirps. The gain of the SOA also affects its refractive index, thus triggering self-phase modulation (SPM). This results in red shift and chirp changes in the pulse spectrum[28]. The chirp change and red shift caused by the refractive index change can account for the pulse width change in the previous research[19,23,25]. However, the pulse width variation due to the refractive index change is usually not exceeding 5 ps, while the pulse duration can be tuned from 4 ps to 30 ps in the experiment. Moreover, SPM usually leads to an increase in pulse width as the current increases, which is contrary to the results of this experiment. Therefore, some other reasons affected the pulse width besides the SPM.

In this experiment, in addition to the SOA current, the rotation of PC also can result in variation of the pulse waveform and pulse width. Autocorrelation curves were measured under different PC states and different currents in the SOA at a repetition rate of 2.5 GHz, respectively. As shown in Fig. 7, with the change of PC state, the pulse width at 500 mA current changes from 4.4 ps to 45.8 ps; in contrast, the pulse width at 190 mA current changes from 25.2 ps to 11.4 ps. It can be seen that the pulse width change is largely related to the polarization state. The polarization state of the light changed for the NPR effect of the SOA when the light passed through the SOA. MZIM is a polarization sensitive device whose modulation depth is greatly affected by the polarization state of the light. When the repetition frequency of the modulated signal is 2.5 GHz and the SNR is 60 dB, the SNR of the modulated light can be changed from 50 dB to 3 dB by changing the polarization state of the injected laser. The modulation depth has a great influence on the pulse width, and the pulse width can be tuned by changing the modulation depth[23,25]. As shown in Fig. 7, the pulse width increased from 4.4 ps to 45.8 ps with the PC state changing, while the modulation depth decreased obviously.

An experiment was designed to verify that changing the SOA current can change the polarization state of the output light.

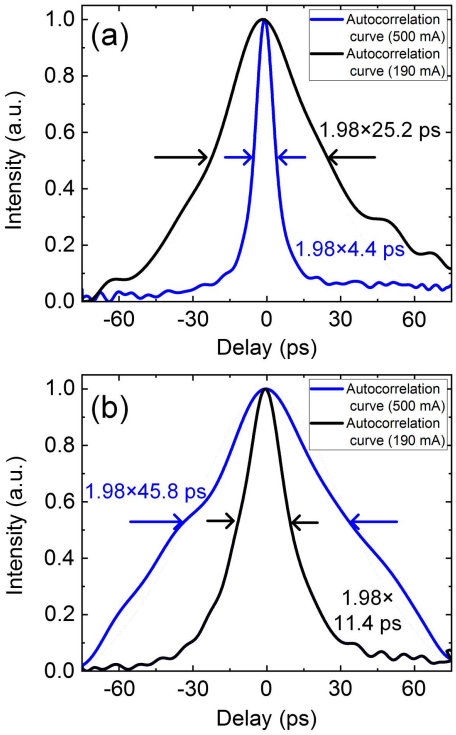

Fig. 7. Pulse width under different PC states at 2.5 GHz repetition rate. The blue line represents the SOA current of 500 mA, and the black line represents the SOA current of 190 mA.

Figure 8 shows the schematic diagram of the experimental setup. A 1550 nm distributed feedback laser with an output power of 5 mW was connected to the input port of the SOA, and the output beam of the SOA was coupled into a PBS through a collimator. The laser passing through the PBS was split into two beams with different polarization states, i.e., P-polarized light and S-polarized light. Recording the intensities of the two lights under different SOA currents, Fig. 9 shows the intensity changes of P-polarized light, S-polarized light, and total laser light when the current changes. As the current increases, the gain of the SOA

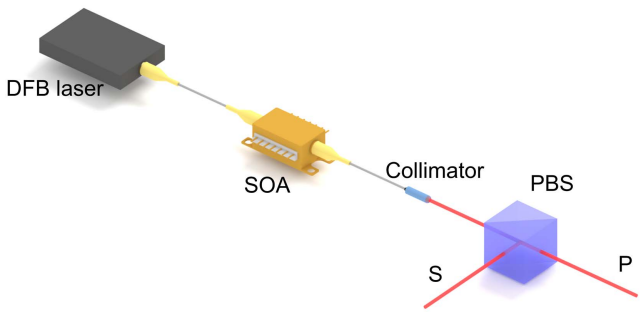

Fig. 8. Schematic diagram of the experiment setup investigating the influence of SOA on the laser polarization state. DFB laser, distributed feedback laser; SOA, semiconductor optical amplifier; PBS, polarization beam splitter; P, P-polarized light; S, S-polarized light.

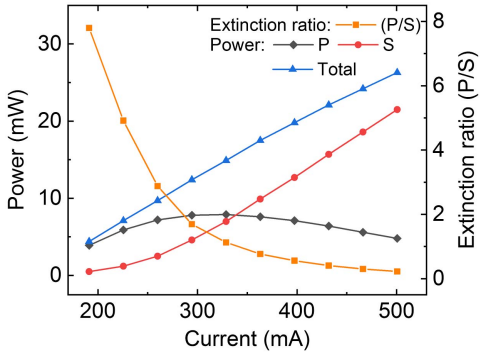

Fig. 9. Trends of the power of P-polarized light, S-polarized light, and extinction ratio (P/S) with current change.

increases, so the total laser light increases linearly. What is more, Fig. 9 shows the variation of the extinction ratio of the output light (the ratio of optical powers of P-polarized light and S-polarized light, P/S) as the current changes. It can be seen that the polarization extinction ratio decreases with the SOA current increasing, which indicates that SOA current can affect the polarization state of the laser in the experiment. Therefore, based on the results shown in Figs. 7 and 9, the polarization state of the laser changes when adjusting the SOA current. The change of the laser polarization state leads to the variation of the modulation depth of the modulator, which finally affects the pulse width of the high repetition rate mode-locked laser.

4. Conclusion

In conclusion, a high repetition rate actively mode-locked fiber laser is demonstrated, in which pulse width and repetition rate can be continuously tuned. Especially, the pulse width tunable range exceeds 25 ps at an ultra-high repetition rate. Through the adjustable RF signal source and ODL, the repetition rate within the range from 2 GHz to 6 GHz can be continuously tuned. At the repetition rate of 2.5 GHz, the pulse width adjustment from 4 to 30 ps is demonstrated. The nonlinear polarization of the SOA can be changed by changing the SOA current. The NPR effect of the SOA causes the intracavity light polarization state to change, and finally the pulse width varies based on the polarization sensitivity of the MZIM. We have realized a new type of pulse width tuning method, which can tune the pulse width in a larger range under the ultra-high repetition rate. This study provides new ideas for tunable mode-locked lasers.

Acknowledgement

This work was supported in part by the National Natural Science Foundation of China (Nos. 62075116 and 62075117), Natural Science Foundation of Shandong Province (Nos. ZR2019MF039 and ZR2020MF114), Qilu Young Scholars from Shandong University, and Distinguished Young Scholars from Shandong University.

References

1. Y. Kamba, K. Tei, S. Yamaguchi, J. Enokidani, and S. Sumida, "Efficient UV generation of a Yb-fiber MOPA producing high peak power for pulse durations of from 100 ps to 2 ns," Opt. Express **21**, 25864 (2013).
2. A. Ruehl, A. Marcinkevicius, M. E. Fermann, and I. Hartl, "80 W, 120 fs Yb-fiber frequency comb," Opt. Lett. **35**, 3015 (2010).
3. H. Kalaycıoğlu, P. Elahi, Ö. Akçaalan, and F. Ö. Ilday, "High-repetition-rate ultrafast fiber lasers for material processing," IEEE J. Sel. Top. Quantum Electron. **24**, 8800312 (2018).
4. R. J. De Young and N. P. Barnes, "Profiling atmospheric water vapor using a fiber laser lidar system," Appl. Opt. **49**, 562 (2010).
5. M. Wang, M. Liu, Y. Chen, D. Ouyang, J. Zhao, J. Pei, and S. Ruan, "Stable noise-like pulse generation in all-PM mode-locked Tm-doped fiber laser based on NOLM," Chin. Opt. Lett. **19**, 091402 (2021).
6. P. Zhang, W. Fan, X. Wang, and Z. Lin, "Generation of 8.5-nJ pulse from all-fiber dispersion compensation-free Yb-doped laser," Chin. Opt. Lett. **8**, 768 (2010).
7. H. Cheng, W. Wang, Y. Zhou, T. Qiao, W. Lin, Y. Guo, S. Xu, and Z. Yang, "High-repetition-rate ultrafast fiber lasers," Opt. Express **26**, 16411 (2018).
8. J. Qin, R. Dai, Y. Li, Y. Meng, Y. Xu, S. Zhu, and F. Wang, "20 GHz actively mode-locked thulium fiber laser," Opt. Express **26**, 25769 (2018).
9. H. Chen, S. P. Chen, Z. F. Jiang, K. Yin, and J. Hou, "All fiber actively mode-locked ytterbium-doped laser with large range temporal tunability," IEEE Photon. Technol. Lett. **26**, 1786 (2014).
10. B. N. Nyushkov, S. M. Kobtsev, A. K. Komarov, and A. K. Dmitriev, "SOA fiber laser mode-locked by gain modulation," J. Opt. Soc. Am. B **35**, 2582 (2018).
11. G. R. Lin, I. H. Chiu, and M. C. Wu, "1.2-ps mode-locked semiconductor optical amplifier fiber laser pulses generated by 60-ps backward dark-optical comb injection and soliton compression," Opt. Express **13**, 1008 (2005).
12. G. R. Lin, Y. S. Liao, and G. Q. Xia, "Dynamics of optical backward-injection-induced gain-depletion modulation and mode locking in semiconductor optical amplifier fiber lasers," Opt. Express **12**, 2017 (2004).
13. J. J. Kang, C. K. Lee, Y. H. Lin, and G. R. Lin, "Chirp evolution algorithm of a dark-optical-comb injection mode-locked SOA fiber laser pulses during soliton compression," IEEE J. Sel. Top. Quantum Electron. **20**, 8 (2013).
14. S. Yan, J. G. Zhang, and W. Zhao, "SOA-based actively mode-locked fiber ring laser by forward injecting an external pulse train," Opt. Commun. **283**, 87 (2010).
15. F. Wang, X. Zhang, E. Xu, and Y. Zhang, "Tunable 19×10 GHz L-band FP-SOA based multi-wavelength mode-locked fiber laser," Opt. Commun. **283**, 1434 (2010).
16. S. Yan, J. Zhang, and W. Zhao, "40-GHz wavelength tunable mode-locked SOA-based fiber laser with 40-nm tuning range," Chin. Opt. Lett. **6**, 676 (2008).
17. Z. Li, X. Yang, E. Tangdiongga, H. Ju, G. D. Khoe, H. J. S. Dorren, and D. Lenstra, "Simulation of mode-locking by nonlinear polarization rotation in a semiconductor optical amplifier," IEEE J. Quantum Electron. **41**, 808 (2005).
18. G. R. Lin, M. C. Wu, and Y. C. Chang, "Suppression of phase and supermode noise in a harmonic mode-locked erbium-doped fiber laser with a semiconductor-optical-amplifier-based high-pass filter," Opt. Lett. **30**, 1834 (2005).
19. I. Evans, C. O'Riordan, M. J. Connelly, L. P. Barry, A. M. Clarke, and P. M. Anandarajah, "Investigation of noise suppression, pulse intensity and chirp of an actively mode-locked semiconductor fiber ring laser," Opt. Commun. **280**, 142 (2007).
20. F. Quinlan, S. Gee, S. Ozharar, and P. J. Delfyet, "Ultralow-jitter and -amplitude-noise semiconductor-based actively mode-locked laser," Opt. Commun. **31**, 2870 (2006).
21. F. Wang, G. Q. Xia, and Z. M. Wu, "Numerical study of a mode-locked fiber ring laser consisting of two SOAs," Proc. SPIE **6352**, 63522 (2006).
22. M. C. Wu, Y. C. Chang, and G. R. Lin, "Comparison on the noise and jitter characteristics of harmonic injection-locked and mode-locked erbium-doped fiber lasers," Proc. SPIE **5623**, 643 (2005).
23. S. Aleksic and V. Krajinovic, "Pulsewidth and chirp of SOA-EAM ring mode-locked lasers," in *IFIP Working Conference on Optical Network Design & Modelling* (2004), p. 293.
24. L. Zhang, X. Wang, X. Li, and H. Liu, "Output pulse width of mode-locked ring laser based on Er^{3+}-doped fiber amplifier and semiconductor optical amplifier," IET Optoelectron. **9**, 10 (2014).
25. C. Peng, M. Yao, J. Zhang, H. Zhang, Q. Xu, and Y. Gao, "Theoretical analyses on short-term stability of semiconductor fiber ring lasers," Opt. Commun. **209**, 181 (2002).
26. Q. Xu and M. Yao, "Ultrahigh supermode noise suppressing ratio of a semiconductor optical amplifier filtered harmonically mode-locked erbium-doped fiber laser," IEEE J. Quantum Electron. **39**, 1260 (2003).
27. G. R. Lin, M. C. Wu, Y. C. Chang, and C. L. Pan, "Ultrahigh supermode noise suppressing ratio of a semiconductor optical amplifier filtered harmonically mode-locked erbium-doped fiber laser," Opt. Express **13**, 7215 (2005).
28. G. P. Agrawal and N. A. Olsson, "Self-phase modulation and spectral broadening of optical pulses in semiconductor laser amplifiers," IEEE J. Quantum Electron. **25**, 2297 (1989).
29. J. Romero-Vivas, L. Krzczanowicz, A. Meehan, and M. J. Connelly, "Dynamic power and chirp measurements of amplified 19 ps pulses in traveling-wave and reflective semiconductor optical amplifiers using a linear pulse characterization technique," Opt. Quantum Electron. **51**, 248 (2019).
30. S. H. Kim, J. R. Ro, B. S. Yoo, and H. H. Park, "Transmission performances of chirp-controlled long-wavelength VCSELs using semiconductor optical amplifier," in *The 6th International Conference on Advanced Communication Technology* (2004), p. 283.
31. W. Kobayashi, M. Arai, T. Fujisawa, T. Sato, T. Ito, K. Hasebe, S. Kanazawa, Y. Ueda, T. Yamanaka, and H. Sanjoh, "Novel approach for chirp and output power compensation applied to a 40-Gbit/s EADFB laser integrated with a short SOA," Opt. Express **23**, 9533 (2015).